Document Title:	**Characterization of Designer Drugs: Chemical Stability, Exposure, and Metabolite Identification, Final Summary Overview and Appendix**
Author(s):	**Megan Grabenauer, Katherine N. Moore, Brian F. Thomas**
Document No.:	**249855**
Date Received:	**April 2016**
Award Number:	**2012-R2-CX-K001**

Basic Scientific Research to Support Forensic Science for Criminal Justice Purposes

Characterization of Designer Drugs: Chemical Stability, Exposure, and Metabolite Identification

Final Summary Overview

Submitted via Grants.gov to:
U.S. Department of Justice
Office of Justice Programs
National Institute of Justice
810 Seventh St., NW
Washington, DC 20531

Prepared by:
Megan Grabenauer, Katherine N. Moore, Brian F. Thomas
RTI International
3040 Cornwallis Road
Research Triangle Park, NC 27709-2194

April 30, 2015

Administrative Point of Contact:
Alicia D. Brown
aliciab@rti.org
Phone: 919-541-8826
Fax: 919-541-6624

NIJ Award No. 2012-R2-CX-K001
RTI Proposal No. 020281200.475
RTI Project No. 0213484.000

RTI INTERNATIONAL

Purpose

Designer drugs such as synthetic cannabinoids and cathinones have become increasingly prevalent, as have their health and societal consequences. Most forensic laboratories are not equipped with the analytical research capabilities required to keep up with the rapid turnover of designer drugs being marketed for recreational use. Currently, little is known about the pharmacological and toxicological profiles of these products; the consequences of long-term usage have yet to be studied, and behavioral and metabolic studies have only been performed on a relatively limited number of compounds. Detection of these designer drugs remains a challenge because as bans on specific compounds go into effect, manufacturers rapidly substitute closely related analogs for the newly banned substances, creating a constantly moving analytical target.

The objective of this research is to gain a more thorough understanding of designer drugs with respect to their chemical exposure profiles and biological elimination pathways. The goals of this project were to 1) determine the stability of currently popular designer drugs and identify major degradation products, including pyrolysis products, and 2) identify their major metabolites. In January 2014 the original scope was expanded to include CB1 and CB2 receptor binding studies to determine activity and efficacy of select synthetic cannabinoids containing a tetramethyl cyclopropyl group and their common ring open degradant forms.

Project Design

The project initially focused on compounds from the JWH and AM series of synthetic cannabinoids and expanded to include emerging designer drugs as they became prevalent. Compounds for analysis were chosen by monitoring multiple sources including online user forums, the Forendex Forums, Designer Drugs Online News, which provides notifications on new compounds discovered by European customs agencies, and through discussions with local law

enforcement and forensic laboratory practitioners. For a complete list of compounds analyzed and their structures see Table A-1 in the appendix. Additional identifying information about each compound is listed in Table A-2.

Designer drug compounds were procured from multiple sources (see methods section) and GC-MS spectra were acquired and uploaded to Forendex (http://forendex.southernforensic.org). Compounds underwent one or more of the following analyses: herbal formulations prepared and smoke condensate analyzed, automated pyrolysis at 800˚C, automated pyrolysis at variable temperatures (200-800 ˚C), stability assessment/forced degradation, in vitro metabolism, in vivo metabolism and characterization of urinary metabolites, and cannabinoid (CB1 and CB2) receptor binding. See Table A-3 for a list of which analyses were completed for each compound.

Methods

Additional methodological details are in the appendix.

Stability/Forced Degradation

Stock solutions were prepared in acetonitrile or methanol at concentrations of 0.5-1 mg/mL. Stability samples were prepared by mixing stock solution with water, acidic, basic, and oxidizing solutions (1:1), which were then placed in an environmentally-controlled stability chamber at 25 °C/60 % relative humidity for 24, 48, 72, and 96 hours. Additional samples of the same composition in water were created and stored under elevated temperatures (50 °C ±5).

Metabolism

In vitro

Compounds (10 μM) were incubated at 37 °C in cryopreserved human hepatocytes (pool of 10 donors), with the exception of PB-22 and 5F-PB-22, which were incubated at 100 μM, and JWH-018 and AM2201 at 50 μM . An aliquot of 100 μL was removed and quenched with acetonitrile

containing 0.2% acetic acid at 0, 15, 120, and 180 min (JWH-018, AM2201, PB-22 and 5F-PB-22 stopped at 120 min). A portion of each aliquot was hydrolyzed with Abalone β-D-glucuronidase (≥ 5,000 units).

In vivo

Mice dosed as part of an independent behavioral study were placed in metabolism cages and urine was collected over 24 hrs. Urine from animals dosed with the same compounds was pooled together and extracted using a salting out liquid-liquid extraction (SALLE) method prior to analysis. A portion of each urine pool was hydrolyzed using Abalone β-D-glucuronidase (≥ 5,000 units).

Liquid Chromatography-Mass Spectrometry (LC-MS)

Samples were analyzed using a Waters Synapt G2 HDMS quadrupole time of flight (Q-TOF) mass spectrometer interfaced to a Waters Acquity ultra performance liquid chromatography (UPLC) system (Waters, Milford, MA). Leucine enkephalin was used as a lockmass to correct for mass shifts during acquisition. Liquid chromatography was performed on an Acquity BEH C18 column (1.7 µm 2.1 x 50 mm) connected to a Vanguard BEH C18 pre-column (1.7 µm x 2.1 X 5 mm) and held at 30 °C. Acquired data was analyzed using Waters MassLynx 4.1 with the aid of the Metabolynx application manager. Parent and metabolite reference standards were used for verification when available.

Pyrolysis

An Agilent 7890 gas chromatograph coupled to a 7001B MSD mass selective detector (Agilent Technologies; Santa Clara, CA) controlled by Agilent Masshunter (version B.05.02.1032) software was used for all analyses. A CDS Analytical 5250T pyrolysis autosampler (Oxford, PA) plumbed with independent supplies of helium and another of compressed air (zero grade) was employed to pyrolyze each sample and transfer the products to the gas chromatograph.

An Agilent DB-5MS capillary column (30 m x 0.25 mm x 0.25 μm, Agilent Technologies) was used to separate volatile analytes with a helium carrier gas flow of 1.0 mL/min. Pyroylsis at 800 ˚C was carried out by setting a starting temperature of 50 ˚C. After one second the pyrolysis probe was ramped at 20˚C/sec to 800˚C. An alternate pyrolyzer method was developed to perform pyrolysis at variable temperatures ranging from 200 to 800 ˚C.

Receptor Binding

Affinity at CB_1 and CB_2 receptors was measured using competitive displacement of [^{3}H]-CP55,940. Efficacy was determined using G-protein coupled signal transduction (GTP-γ-[^{35}S]) binding assays.

Results

Detailed results will be disseminated through peer-reviewed publications. For completeness, overall summary tables are provided in the appendix to this Final Summary Overview.

Stability/Forced Degradation

The Stability/Forced degradation results are summarized in Table A-5. The data suggest that for compounds with a tetramethyl cyclopropyl group (e.g. UR-144) exposure to elevated temperatures is a pivotal factor in the ring-opening conversion of the cyclopropyl ring. Synthetic cannabinoid compounds with ester linkages (e.g., PB-22) are susceptible to rapid hydrolysis and transesterification proceeds rapidly in the presence of methanol.

Pyrolysis

Full pyrolysis results at 800˚C are summarized in Table A-6. Of the synthetic cannabinoids studied, only four retained more than 80% of the original dose after pyrolysis: JWH-018 (91%), JWH-018 adamantyl analog (85%), JWH-019 (84%), and THJ-018 (98%). All ester containing synthetic cannabinoids underwent significant thermally-induced structural changes resulting in less

than 5% retention of the original dose: PB-22 (0%), 5F-PB-22 (0%), BB-22 (0%), A-834735 (2%), FDU-PB-22 (3%), and FUB-PB-22 (0%). For all synthetic cannabinoids containing a teramethylcyclopropyl ring substituent, greater than 50% of the original dose was converted to a ring opened form of the parent compound. Dehalogenation was commonly observed for halogen containing compounds. It is likely that users are unknowingly being exposed to novel synthetic cannabinoid structures from thermal degradation and pyrolysis, which may have unique pharmacological properties from the original chemical entities.

Metabolism

ADBICA, ADB-FUBINACA, AB-FUBINACA, ADB-PINACA, AB-PINACA, 5F-AB-PINACA, and 5Cl-AB-PINACA in vitro metabolites

Major metabolic transformations of all of the 1-amino-3-methyl-1-oxobutan-2-yl (AB) and 1-amino-3,3-dimethyl-1-oxobutan-2-yl (ADB) indazole carboxamide compounds studied are hydrolysis of the distal amide and hydrolysis of the distal amide followed by glucuronide conjugation. (See Table A-7). ADBICA was the only 1-amino-3,3-dimethyl-1-oxobutan-2-yl (ADB) carboxamide compound for which the amide hydrolysis and its glucuronide conjugate were not observed. Unlike the other compounds in Table A-7, ADBICA contains an indole moiety rather than an indazole moiety. It is unknown if this may contribute to the lack of amide hydrolysis as we do not have data on any other indole carboxamide compounds for comparison. Unlike with other metabolites identified in this study, the metabolite resulting from amide hydrolysis elutes after the parent compound while its glucuronide conjugate elutes earlier than the parent compound. Also, n-dealkylation was observed with ADBICA but not the other carboxamide compounds. Again, it is unclear if the indole versus indazole moiety plays a role in this. N-dealkylation was not observed with the compounds in Table A-10 (THJ type compounds) and these also contain an indazole moiety. Compounds with a halogen group (Cl or F) on the terminal alky chain underwent

dehalogenation forming non-unique metabolites. AB-FUBINACA and ADB-FUBINACA were similar to other 4-fluorobenzyl compounds FDU-PB-22 and FUB-PB-22 in that no defluorination was observed.

In vitro metabolites of PB-22, 5-F-PB-22, BB-22, FDU-PB-22, and FUB-PB-22 and in vivo metabolites of PB-22 3-carboxyindole

Major metabolites for all 3-indole ester-linked compounds studied were the 3-carboxyindole and its glucuronide conjugate (see Table A-8). For PB-22, 5-F-PB-22 and BB-22 the presence of 3-carboxyindole may provide evidence that a compound from this class was ingested, but care should be taken to look for other distinctive metabolites because of other compounds that could lead to the 3-carboxyindole metabolite. An example of this is shown with FDU-PB-22 and FUB-PB-22 where the same 3-carboxyindole is identified as a metabolite. Interestingly, FDU-PB-22 and FUB-PB-22 do not undergo defluorination as seen with compounds with terminal fluoroalkyl side chains. They also do not hydroxylate on the 4-fluorobenzyl indole moiety as seen in similar compounds. 5-F-PB-22 undergoes defluorination subsequently forming several metabolites in common with PB-22 metabolites. PB-22 4-hydroxypentyl and PB-22 5-hydroxypentyl co-eluted with the LC method utilized, but at least one of these metabolites was observed for both PB-22 and 5F-PB-22 (defluorinated).

SDB-006, JWH-018 adamantyl analog and JWH-018 adamantyl carboxamide in vitro metabolites

In vitro metabolites for the compounds listed above are summarized in Table A-9. For all compounds, hydroxylation and hydroxylation followed by glucuronide conjugation were the primary metabolic transformations. Both JWH-018 adamantyl analog and JWH-018 adamantyl carboxamide are hydroxylated and glucuronide conjugated on both the adamantly moiety and the 1-pentyl-1*H*-indole moiety, with hydroxylation on the adamantly moiety being the dominant metabolite. Note that beyond hydroxylation, the metabolites for JWH-018 adamantyl analog were low intensity and

characteristic fragment ions were not observed. SDB-006 was the only compound in this table to form a dihydrodiol. This was a minor metabolite and fragment intensity in the high energy mass spectrum was not sufficient to determine the exact location of the modification. SDB-006 was also the only compound to form 3-carboxamide indole.

THJ, 5F-THJ, THJ-018, THJ2201, and AM2201 benzimidazole analog in vitro metabolites and in vivo metabolites for AM2201 benzimidazole analog excreted in urine

All five of these compounds underwent hydroxylation and glucuronide conjugation (Table A-10) which is common among this class of new designer cannabinoids as well as in previous reports for the original JWH type compounds. These THJ type compounds all also form dihydrodiols, regardless of whether they are naphthalene or quinonline type compounds. This is similar to reports in the literature for the original JWH type compounds that typically have a naphthalene moiety. However, in the THJ type compounds, these are only minor metabolites. Like all of the compounds in this study, the parent compound was detected in the in vitro samples even at 3h. The fluorinated compounds underwent defluorination forming THJ and THJ-018 metabolites. Carboxylation of THJ was not observed, even when searching for common fragment ions, but it was observed in 5F-THJ after defluorination. Interestingly, for THJ2201 and AM2201 benzimidazole analog we observe what could possibly be saturation at the carbonyl, which was not detected for any of the other compounds with similar structures. More investigation into this is needed. Also, N-dealkylation of the pentyl chain was not observed for these compounds. It may be due to the presence of an indazole moiety versus an indole moiety, or since it is typically a minor uncharacteristic metabolite, the intensity may be too low to observe in these cases.

Cyclopropyl ketone indole in vitro metabolites for degradant and non-degradant compounds and in vivo metabolites for the degradant compounds.

As summarized in Table A-11, all of these compounds undergo hydroxylation followed by glucuronidation. Other oxidative metabolites such as dihydroxlation, and carboxylation were also observed. Hydoxylation occurs on the 1-(tetrahydro-2*H*-pyran-4-ylmethyl)-1*H*-indole unlike the 1-(4-fluorobenzyl)-1-*H*-indole compounds (e.g. ADB-FUBINACA, AB-FUBINACA, FDU-PB-22 and FUB-PB-22) that do not form hydroxylations on that moiety. UR-144, XLR-11, and their degradants underwent N-dealkylation of the alky pentyl and 5-fluoro alky pentyl side chain. Care must be taken when choosing distinctive biotransformations to monitor for the presence of these compounds since XLR-11 and its degradant undergo defluorination forming UR-144 and UR-144 degradant specific metabolites.

Receptor Binding

CB_1 and CB_2 receptor affinities of the ring-open degradants of XLR-11 and UR-144 were determined. These ring-opened analogs retained nM affinity and act as full agonists at both the CB_1 and CB_2 receptors, as do their non-degraded, parent compounds. However, the thermal degradation product and biological metabolite observed with PB-22 (1-pentyl-1H-indole-3-carboxylic acid) was unable to alter GTP-γ-S binding at doses up 1000-fold higher than active concentrations of PB-22. The XLR-11 degradant displaced [^{3}H]CP55,940 from the CB_1 receptor, with an apparent Ki of 5.0 ± 0.57 nM and from the CB_2 receptor with an apparent Ki of 0.9 ± 0.13 nM. The UR-144 degradant displaced [^{3}H]CP55,940 from the CB_1 receptor with an apparent K_i of 11.23 ± 2.54 nM and from the CB_2 receptor with an apparent K_i of 1.54 ± 0.21 nM. Notably, the degradants of each compound showed at least 2-fold lower affinity for both cannabinoid receptors than shown previously for the parent compounds, which in turn, had at least 2-fold lower affinity than Δ^9-THC. Because smoking or vaporizing results in increased exposure to the ring opened degradant compounds compared to the

parent compounds, cannabimimetic potency is predicted to be greater in human users than the CB_1 affinities of XLR-11 and UR-144 would suggest.

Scholarly Products

Detailed results have been presented within 8 conference presentations. See table A-12 in the Appendix for full list of these presentations.

Publications

Wiley, JL, Marusich, JA, Lefever, TW, Grabenauer, M, Moore, KN, Thomas, BF. 2013. Cannabinoids in Disguise: Δ^9-Tetrahydrocannabinol-Like Effects of Tetramethylcyclopropyl Ketone Indoles. *Neuropharmacology*. 75, 145-154

Planned Publications

- Wiley, JL, Marusich, JA, Lefever, TW, Antonazzo, KR, Wallgren, MT, Cortes, RA, Patel, PR, Grabenauer, M, Moore, KN, Thomas, BF. 2015 All That Glitters Is Not (Spice) Gold: Dissociation Between Affinity and Potency of Novel Synthetic Cannabinoids in Producing Δ^9-Tetrahydrocannabinol-Like Effects in Mice. Submitted 4/2015 to Journal of Pharmacology and Experimental Therapeutics.

- Manuscript joint with Jenny Wiley's group with mouse in vivo metabolites of JWH-073, JWH-018, JWH-081, JWH-391, JWH-210, AM-2201, JWH-167, combined with behavioral data from the dosed animals.

- Manuscript on 5F-AKB48 found in Spice samples from Richland County. Homogeneity of packages of samples. This manuscript is in the final stages of editing prior to submission to the Journal of Forensic Sciences (JFS).

- Manuscript on pyrolysis survival and binding affinity for UR-144, XLR-11, PB-22 (content of poster presented at SOFT). This manuscript will be targeted for a high profile journal with a more general audience such as the Journal of the American Chemical Society (JACS).

- Manuscript on metabolites of structurally related synthetic cannabinoids (content of poster presented at SOFT) This manuscript will be targeted for the forensic toxicology community specifically, with a planned submission to the Journal of Analytical Toxicology (JAT).

- Manuscript comparing mouse in vivo metabolites and human hepatocyte in vitro metabolites. This manuscript will be targeted for a more general analytical chemistry audience such as the readership of Analytical Chemistry (Anal Chem).

Implications for Policy and Practice

Through this research we identified metabolites suitable as potential markers of use, degradation products, and pyrolysis products that may be left in an ash residue to use for confirmation of the presence of parent compound. The dataset is extensive and is a reliable starting point for forensic laboratories across the United States to develop assays for detection of use, as well as confirmation of the presence of parent compound within residues. New designer drugs are still coming to market, faster than targeted testing can keep up. However, within each class of designer drugs, the elements of chemical structure and design often follow known or rational substitution patterns required to enhance or retain pharmacological activity. By performing a thorough and systematic study looking at families of structurally related compounds, we are able to predict markers for broad classes of compounds, such as aminoalkylindole cannabinoids or phenethylamines, and help practitioners keep up with designer drug manufacturers.

We have shown that depending on the sample preparation technique and route of administration, the compound a person is exposed to may not be the compound originally intended. We have provided the forensic toxicology community with information about known degradation and pyrolysis products and major metabolites that should be included as candidates when searching for markers of use. Armed with this knowledge, these compounds are less likely to go undetected. Knowing conditions under which compounds are likely to degrade will impact sample handling, extraction, and analytical methods employed in sample preparation and forensic analyses, especially for compounds that were found to be particularly labile.

Appendix to Final Summary Overview
Award No. 2012-R2-CX-K001

Table A - 1 Structures of Compounds Analyzed

Note: compounds are listed by common name and ordered based on structural similarity

Common Name	Structure	Monoisotopic Mass	$[M+H]^+$
Cannabimimetic Compounds			
JWH-018	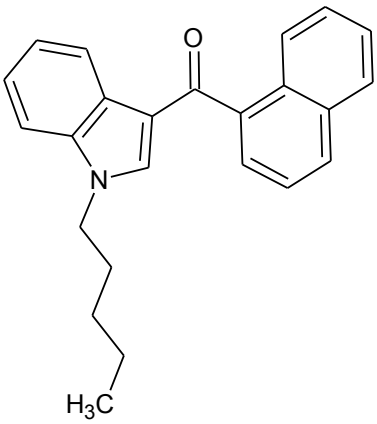	341.1780	342.1852
AM-2201	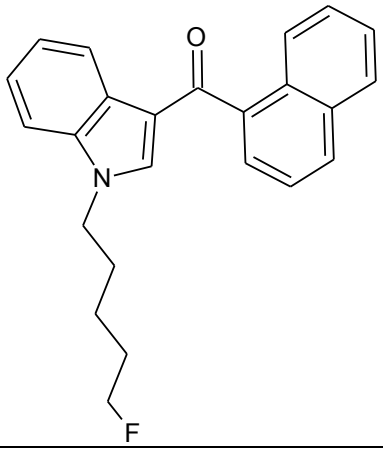	359.1685	360.1758

Common Name	Structure	Monoisotopic Mass	$[M+H]^+$
MAM-2201	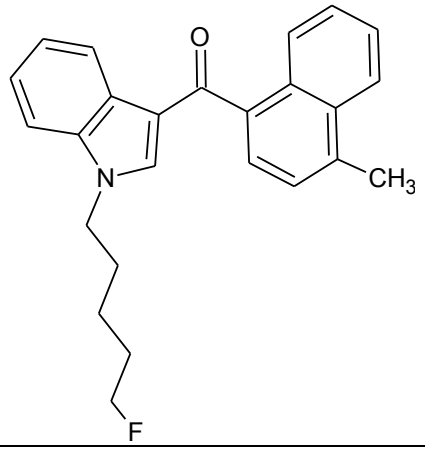	373.1841	374.1915
EAM-2201	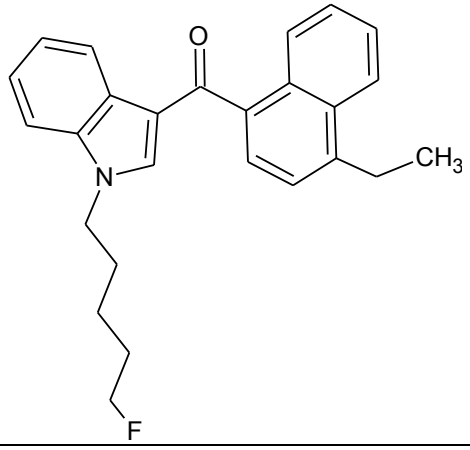	387.1998	388.2071
JWH-018 adamantyl analog	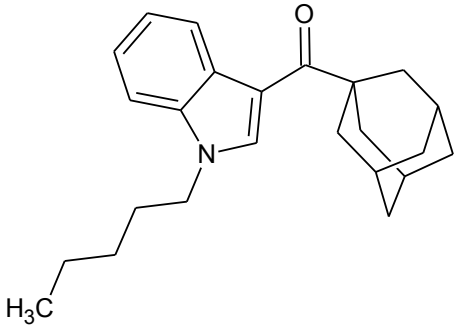	349.2406	350.2478

Common Name	Structure	Monoisotopic Mass	$[M+H]^+$
JWH-018 adamantyl carboxamide	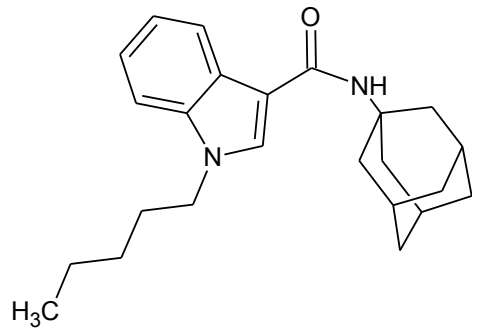	364.2515	365.2587
STS-135	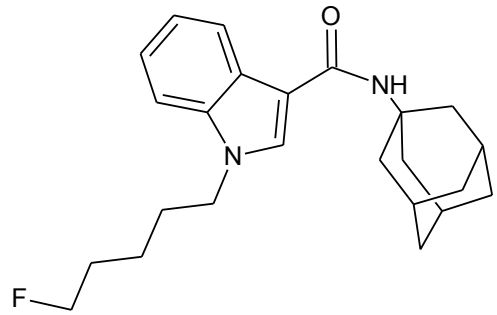	382.2420	383.2493
AKB48	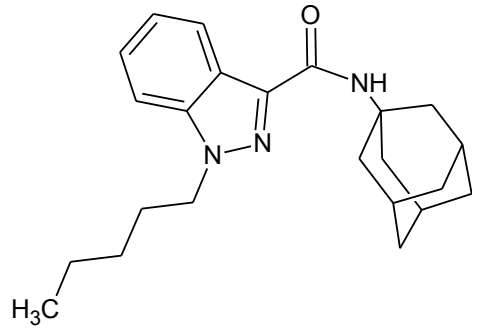	365.2467	366.2540

Common Name	Structure	Monoisotopic Mass	$[M+H]^+$
UR-144	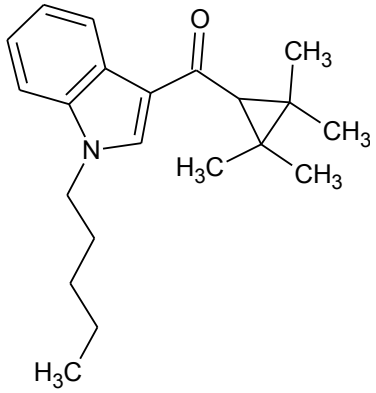	311.2249	312.2322
UR-144 Degradant	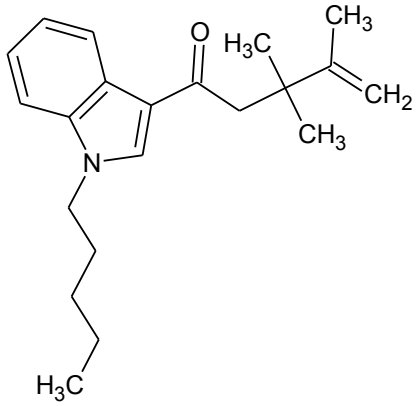	311.2249	312.2322
5-Bromo UR-144	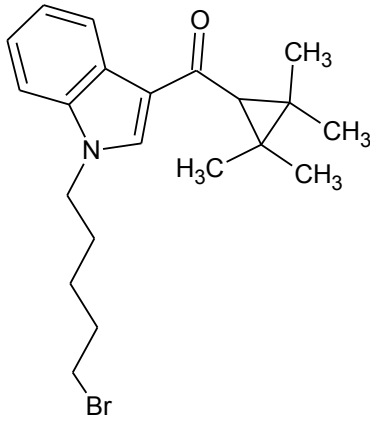	389.1354	390.1426

Common Name	Structure	Monoisotopic Mass	$[M+H]^+$
5-Chloro UR-144	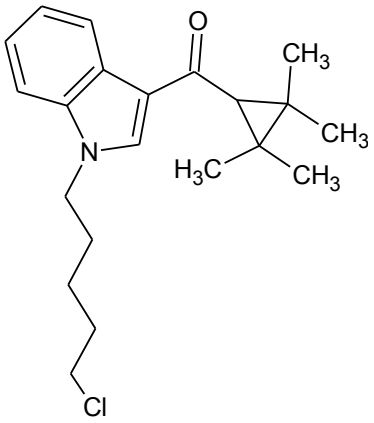	345.1859	346.1932
XLR-11	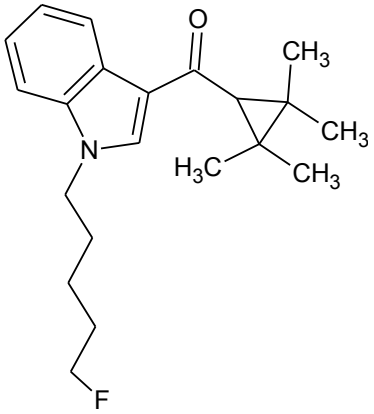	329.2155	330.2228
XLR-11 degradant	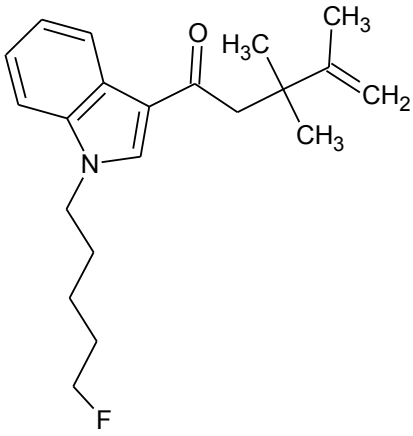	329.2155	330.2228

Common Name	Structure	Monoisotopic Mass	$[M+H]^+$
XLR-11 N-(4-pentenyl) analog	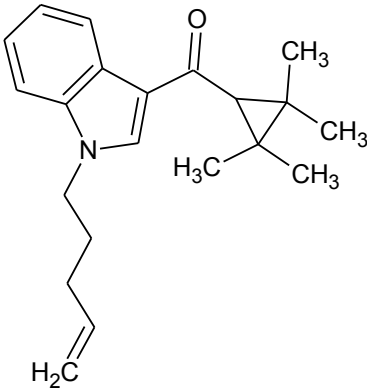	309.2092	310.2165
A-834,735	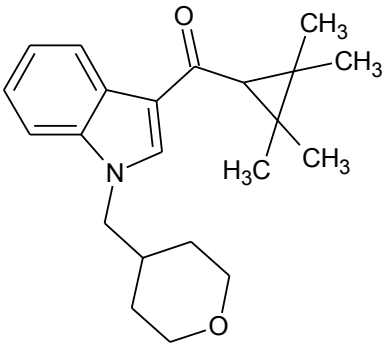	339.2198	340.2271
A-834,735 degradant	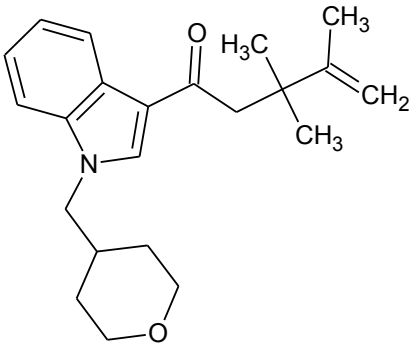	339.2198	340.2271

Common Name	Structure	Monoisotopic Mass	$[M+H]^+$
PB-22	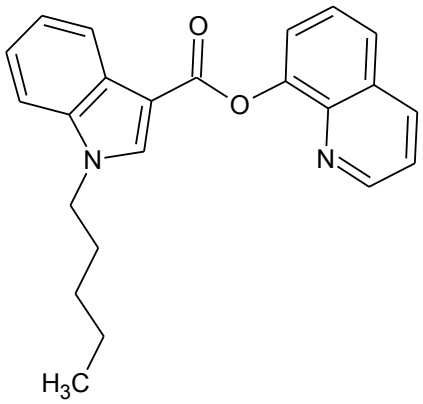	358.1681	359.1754
PB-22 3-carboxy indole	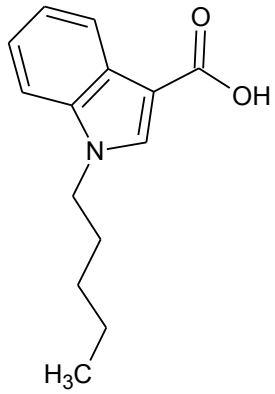	231.1259	232.1332
5F-PB-22	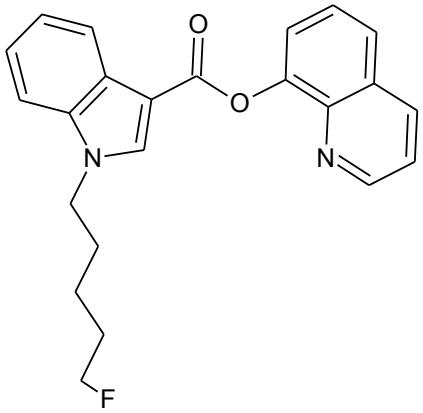	376.1587	377.1659

Common Name	Structure	Monoisotopic Mass	$[M+H]^+$
FUB-PB-22	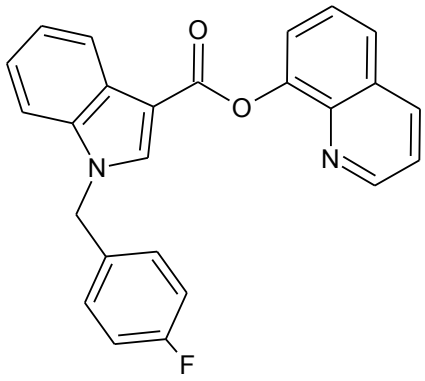	396.1274	397.1346
FDU-PB-22	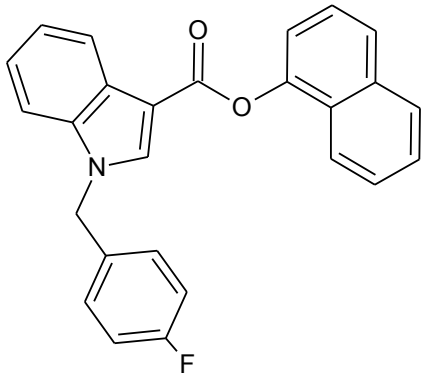	395.1321	396.1394
BB-22	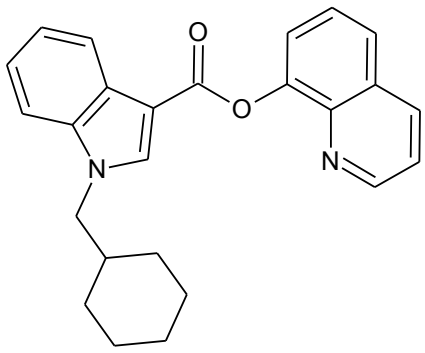	384.1838	385.1911

Common Name	Structure	Monoisotopic Mass	$[M+H]^+$
ADBICA	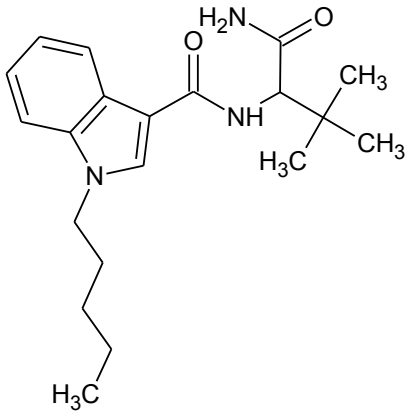	343.2260	344.2333
AB-PINACA	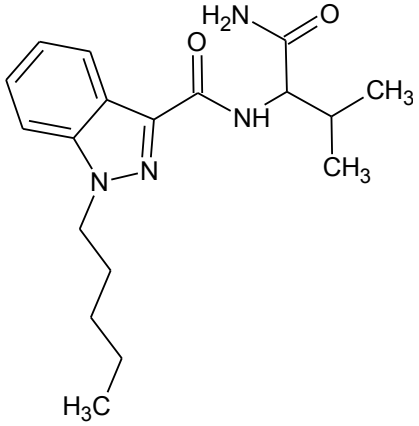	330.2056	331.2129
5F-AB-PINACA	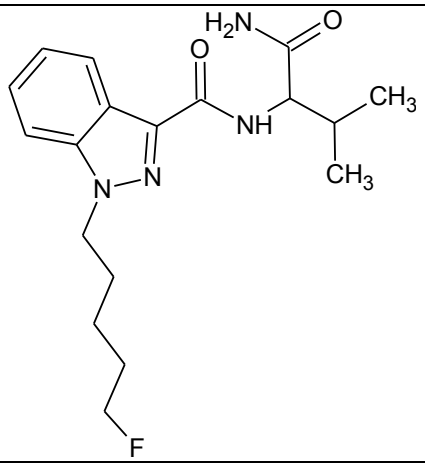	348.1961	349.2034

Common Name	Structure	Monoisotopic Mass	$[M+H]^+$
5-Chloro-AB-PINACA	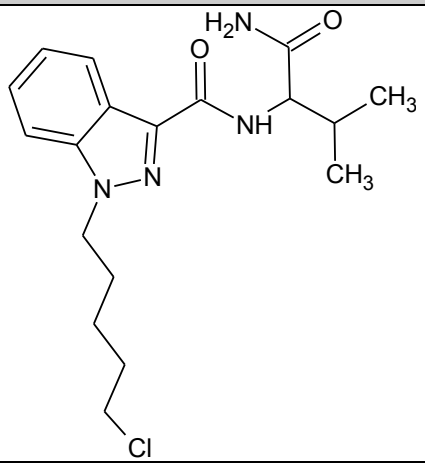	364.1666	365.1739
ADB-PINACA	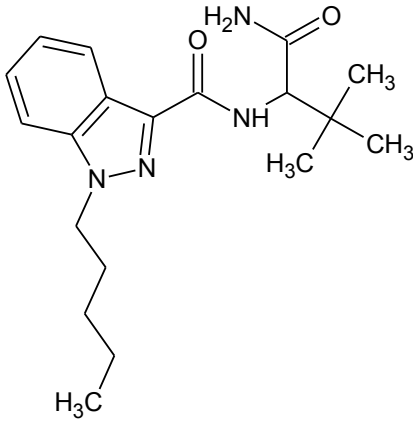	344.2212	345.2285
AB-CHMINACA	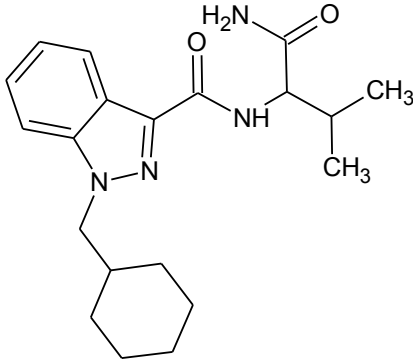	356.2212	357.2285

Common Name	Structure	Monoisotopic Mass	$[M+H]^+$
AB-FUBINACA	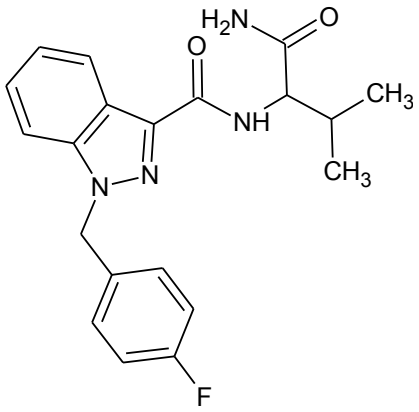	368.1649	369.1721
ADB-FUBINACA	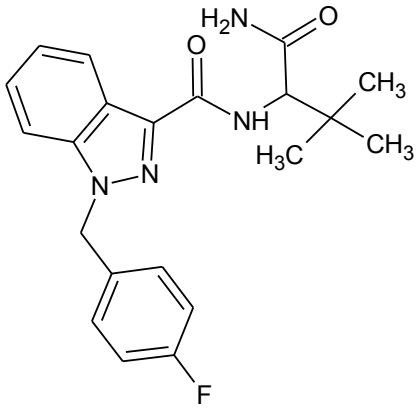	382.1805	383.1877
THJ 018	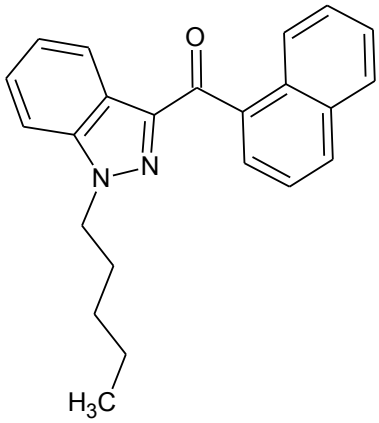	342.1732	343.1805

Common Name	Structure	Monoisotopic Mass	$[M+H]^+$
THJ 2201	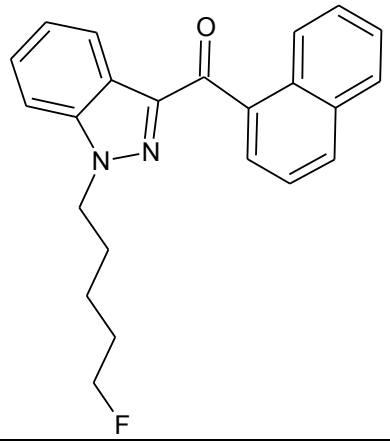	360.1638	361.1711
AM2201 benzimidazole analog	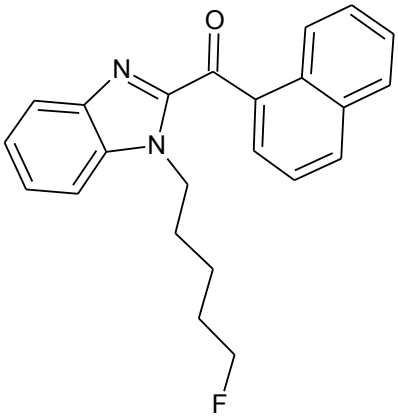	360.1638	361.1711
NNEI	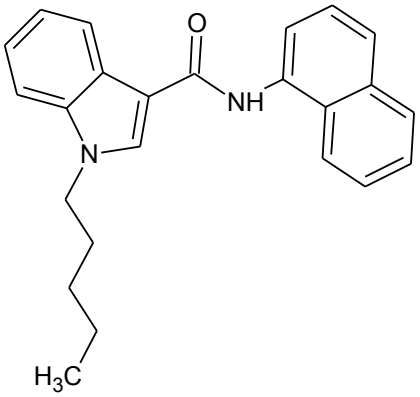	356.1888	357.1961

Common Name	Structure	Monoisotopic Mass	$[M+H]^+$
MN-18	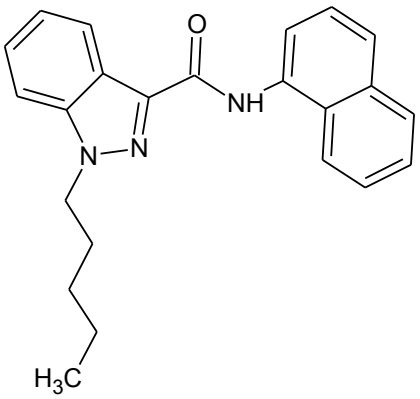	357.1841	358.1913
THJ	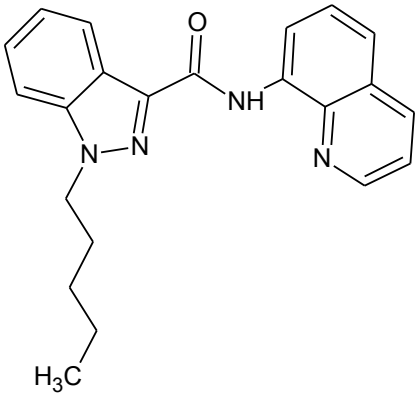	358.1794	359.1866
5F-THJ	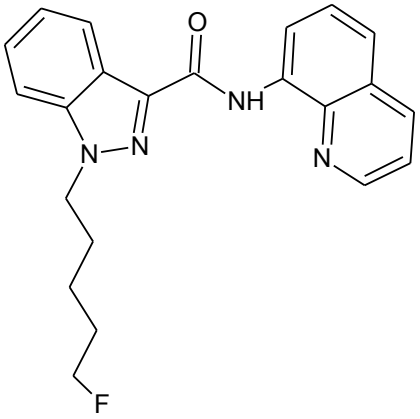	376.1699	377.1772

Common Name	Structure	Monoisotopic Mass	$[M+H]^+$
EG-018	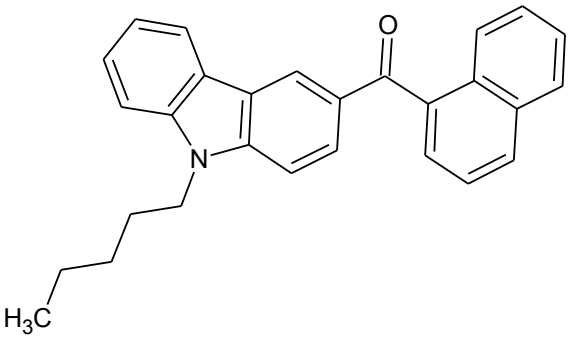	391.1936	392.2009
SDB-006	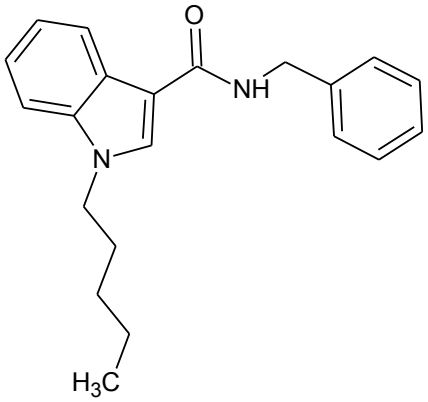	320.1889	321.1961
Synthetic Cathinone, Phenethylamine, Indane, and Piperazine Compounds			
Flephedrone	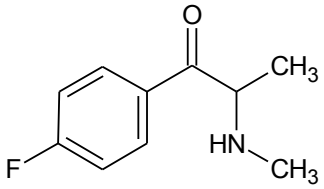	181.0903	182.0976

Common Name	Structure	Monoisotopic Mass	$[M+H]^+$
Alpha-Ethylaminopentiophenone	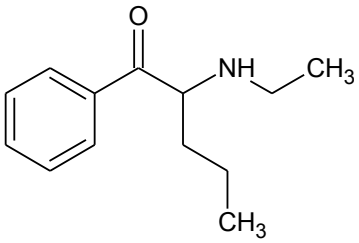	205.1467	206.1539
NRG-3	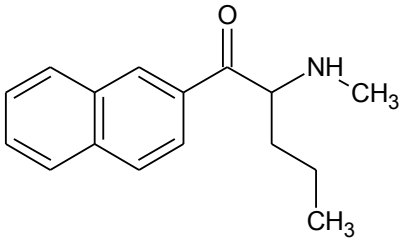	241.1467	242.1539
4-MeO-alpha-PVP	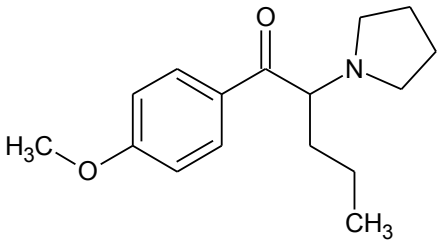	261.1729	262.1802

Common Name	Structure	Monoisotopic Mass	$[M+H]^+$
4-MePPP	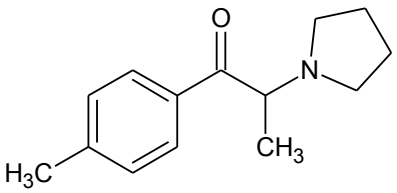	217.1467	218.1539
Alpha-PVT	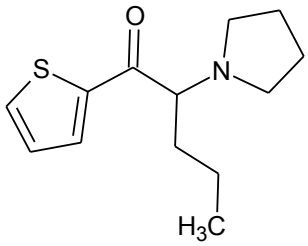	237.1187	238.1260
25I-NBOME	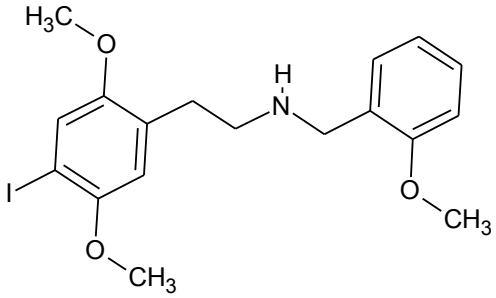	427.0644	428.0717

Common Name	Structure	Monoisotopic Mass	$[M+H]^+$
2C-N	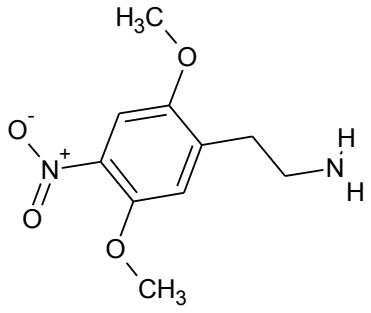	226.0953	227.1026
MDAI	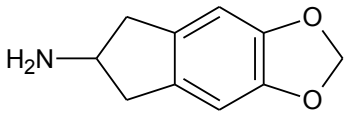	177.0790	178.0862
2-AI	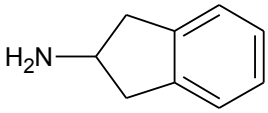	133.0891	134.0964

Common Name	Structure	Monoisotopic Mass	$[M+H]^+$
BZP	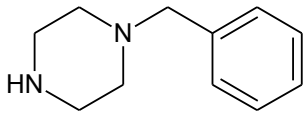	176.1313	177.1386
TFMPP	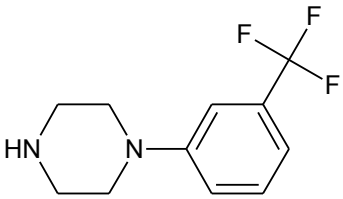	230.1031	231.1104

Table A - 2 Compound Identities

Common Name	Synonyms	Systematic Name	InChI Key	CAS Number (if applicable)
Cannabimimetic Compounds				
JWH-018	AM678	1-Pentyl-3-(1-naphthoyl)indole	JDNLPKCAXICMBW-UHFFFAOYSA-N	209414-07-3
AM-2201		1-(5-Fluoropentyl)-3-(1-naphthoyl) indole	ALQFAGFPQCBPED-UHFFFAOYSA-N	335161-24-5
MAM-2201		1-(5-Fluoropentyl)-3-(4-methyl-1-naphthoyl) indole	IGBHZHCGWLHBAE-UHFFFAOYSA-N	1354631-24-5
EAM-2201		1-(5-Fluoropentyl)-3-(4-ethyl-1-naphthoyl) indole	NSCXPXDWLZORPX-UHFFFAOYSA-N	1364933-60-7
JWH-018 adamantyl analog	AB-001	1-Pentyl-3-(1-adamantoyl)indole	SHWDYCMMUPPWQM-AECLTTBISA-N	1345973-49-0
JWH-018 adamantyl carboxamide	APICA, 2NE1, SDB-001	*N*-Adamantyl-1-pentyl-1*H*-indole-3-carboxamide	MDJYHWLDDJBTMX-YGMNDUCWSA-N	1345973-50-3
STS-135	4-Fluoro-APICA	N-adamantyl-1-fluoropentylindole-3-Carboxamide	COYHGVCHRRXECF-YGMNDUCWSA-N	1354631-26-7
AKB48	APINACA	N-(1-Adamantyl)-1-pentyl-1H-indazole-3-carboxamide	UCTCCIPCJZKWEZ-XHICYHHKSA-N	1345973-53-6
UR-144	KM-X1	1-Pentyl-1H-indol-3-yl)(2,2,3,3-tetramethylcyclopropyl)methanone	NBMMIBNZVQFQEO-UHFFFAOYSA-N	1199943-44-6
UR-144 degradant		3,3,4-trimethyl-1-(1-pentyl-1H-indol-3-yl)pent-4-en-1-one	NBJHWTCAQOYUND-UHFFFAOYSA-N	N/A
5-Bromo-UR-144		(1-(5-bromopentyl)-1H-indol-3-yl)(2,2,3,3-tetramethylcyclopropyl)methanone	HEWSXAZQMCDEMO-UHFFFAOYSA-N	N/A
5-Chloro-UR-144		(1-(5-chloropentyl)-1H-indol-3-yl)(2,2,3,3-tetramethylcyclopropyl)methanone	CKIOITGXSRFWIS-UHFFFAOYSA-N	1445577-42-3
XLR-11	5-Fluoro-UR-144	1-(5-Fluoro-pentyl)1H-indol-3-yl](2,2,3,3-tetramethylcyclopropyl)methanone	PXLDPUUMIHVLEC-UHFFFAOYSA-N	1364933-54-9
XLR-11 degradant		1-(1-(5-fluoropentyl)-1H-indol-3-yl)-3,3,4-trimethylpent-4-en-1-one	BEZVSTOQIZTNCK-UHFFFAOYSA-N	N/A
XLR-11 N-(4-pentenyl) analog		(1-(pent-4-en-1-yl)-1H-indol-3-yl)(2,2,3,3-tetramethylcyclopropyl)methanone	NXTLUQFOTQPMOD-UHFFFAOYSA-N	1445578-20-0
A-834,735		[1-[(tetrahydro-2H-pyran-4-yl)methyl]-1H-indol-3-yl](2,2,3,3-tetramethylcyclopropyl)-methanone	NQTMRZNYLIGQCF-UHFFFAOYSA-N	895155-57-4

Common Name	Synonyms	Systematic Name	InChI Key	CAS Number (if applicable)
A-834,735 degradant		,3,4-trimethyl-1-(1-((tetrahydro-2H-pyran-4-yl)methyl)-1H-indol-3-yl)pent-4-en-1-one	SHMFIOCKSMJXSG-UHFFFAOYSA-N	N/A
PB-22	QUPIC	Quinolin-8-yl 1-pentyl-1H-indole-3-carboxylate	ZAVGICCEAOUWFM-UHFFFAOYSA-N	1400742-17-7
PB-22 3-carboxyindole		1-pentyl-1H-indole-3-carboxylic acid	HAPJUNILBCTRIJ-UHFFFAOYSA-N	727421-73-0
5F-PB-22	5-Fluoro QUPIC	Quinolin-8-yl 1-(5-fluoropentyl)-1H-indole-3-carboxylate	MBOCMBFDYVSGLJ-UHFFFAOYSA-N	1400742-41-7
FUB-PB-22		Quinolin-8-yl-1-(4-fluorobenzyl)-1H-indole-3-carboxylate	ROHVURVXAOMRJY-UHFFFAOYSA-N	N/A
FDU-PB-22		Naphthalen-1-yl 1-(4-fluorobenzyl)-1H-indole-3-carboxylate	RCEKSVIFQKKFLS-UHFFFAOYSA-N	N/A
BB-22	QUCHIC	1-(cyclohexylmethyl)-8-quinolinyl ester-1H-indole-3-carboxylic acid	RHYGTJXOHOGQGI-UHFFFAOYSA-N	1400742-42-8
ADBICA		N-(1-amino-3,3-dimethyl-1-oxobutan-2-yl)-1-pentyl-1H-indole-3-carboxamide	IXUYMXAKKYWKRG-UHFFFAOYSA-N	1445583-48-1
AB-PINACA		N-(1-amino-3-methyl-1-oxobutan-2-yl)-1-pentyl-1H-indazole-3-carboxamide	GIMHPAQOAAZSHS-HNNXBMFYSA-N	1445752-09-9
5F-AB-PINACA		N-(1-amino-3-methyl-1-oxobutan-2-yl)-1-(5-fluoropentyl)-1H-indazole-3-carboxamide	WCBYXIBEPFZUBG-HNNXBMFYSA-N	N/A
5-Chloro-AB-PINACA		N-(1-amino-3-methyl-1-oxobutan-2-yl)-1-(5-chloropentyl)-1H-indazole-3-carboxamide	VUPMALPMUYUYES-UHFFFAOYSA-N	N/A
ADB-PINACA		N-(1-amino-3,3-dimethyl-1-oxobutan-2-yl)-1-pentyl-1H-indazole-3-carboxamide	FWTARAXQGJRQKN-UHFFFAOYSA-N	N/A
AB-CHMINACA		N-[(1S)-1-(aminocarbonyl)-2-methylpropyl]-1-(cyclohexylmethyl)-1H-indazole-3-carboxamide	KJNZIEGLNLCWTQ-UHFFFAOYNA-N	1185887-21-1
AB-FUBINACA		N-(1-amino-3-methyl-1-oxobutan-2-yl)-1-(4-fluorobenzyl)-1H-indazole-3-carboxamide	AKOOIMKXADOPDA-KRWDZBQOSA-N	1185282-01-2
ADB-FUBINACA		N-[1-(aminocarbonyl)-2,2-dimethylpropyl]-1-[(4-fluorophenyl)methyl]-1H-indazole-3-carboxamide	ZSSGCSINPVBLQD-UHFFFAOYSA-N	1445583-51-6
THJ 018		1-naphthalenyl(1-pentyl-1H-indazol-3-yl)-methanone	VAKGBPSFDNTMDJ-UHFFFAOYSA-N	1364933-55-0
THJ 2201		(1-(5-fluoropentyl)-1H-indazol-3-yl)(naphthalen-1-yl)methanone	DULWRYKFTVFPTL-UHFFFAOYSA-N	N/A

Common Name	Synonyms	Systematic Name	InChI Key	CAS Number (if applicable)
AM2201 benzimidazole analog	FUBIMINA, FTHJ	(1-(5-fluoropentyl)-1H-benzo[d]imidazol-2-yl)(naphthalen-1-yl)methanone	KUESSZMROAFKQJ-UHFFFAOYSA-N	N/A
NNEI	MN-24	N-1-naphthalenyl-1-pentyl-1H-indole-3-carboxamide	GWCQNKRMTGVYIZ-UHFFFAOYSA-N	1338925-11-3
MN-18		N-1-naphthalenyl-1-pentyl-1H-indazole-3-carboxamide	UJKHLVOEXULDRU-UHFFFAOYSA-N	1391484-80-2
THJ		1-pentyl-N-(quinolin-8-yl)-1H-indazole-3-carboxamide	YAYIQXMTUCPLHG-UHFFFAOYSA-N	N/A
5F-THJ		1-(5-fluoropentyl)-N-(quinolin-8-yl)-1H-indazole-3-carboxamide	GMRIDDSOZRLMAN-UHFFFAOYSA-N	N/A
EG-018		naphthalen-1-yl(9-pentyl-9H-carbazol-3-yl)methanone	FJMMDJDPNLZYLA-UHFFFAOYNA-N	N/A
SDB-006		1-pentyl-N-(phenylmethyl)-1H-indole-3-carboxamide	OLACYTSBFXCDOH-UHFFFAOYSA-N	695213-59-3
Synthetic Cathinone, Phenethylamine, Indane, and Piperazine Compounds				
Flephedrone	4-Fluoro-N-methylcathinone , 4-FMC	1-(4-fluorophenyl)-2-(methylamino)propan-1-one	AQIZJTCPVRVBFJ-UHFFFAOYSA-N	7589-35-7
α-Ethylaminopentiophenone		2-(ethylamino)-1-phenyl-1-pentanone	QIVGZMBSFAGAAC-UHFFFAOYSA-N	18268-16-1
NRG-3		2-(methylamino)-1-(naphthalen-2-yl)pentan-1-one	ZGCURDBVAZMAEH-UHFFFAOYSA-N	N/A
4-MeO-α-PVP	4-methoxy-α-Pyrrolidinopentiophenone	1-(4-methoxyphenyl)-2-(1-pyrrolidinyl)-1-pentanone	WPXBEBRLURPPOY-UHFFFAOYSA-N	5537-19-9
4-MePPP	4-methyl-α-pyrrolidinopropiophenone	1-(4-methylphenyl)-2-(pyrrolidin-1-yl)-propan-1-one)	MRWBETWZAYOULZ-UHFFFAOYSA-N	1313393-58-6
α-PVT	α-Pyrrolidinopentiothiophenone	2-(pyrrolidin-1-yl)-1-(thiophen-2-yl)pentan-1-one	RURGIWIREJBFLI-UHFFFAOYSA-N	N/A
25I-NBOME	2C-I-NBOMe, 25I, Cimbi-5	2-(4-iodo-2,5-dimethoxyphenyl)-N-(2-methoxybenzyl) ethanamine	IPBBLNVKGLDTML-UHFFFAOYSA-N	1043868-97-8
2C-N		2-(2,5-Dimethoxy-4-nitro-phenyl)ethanamine	ZMUSDZGRRJGRAO-UHFFFAOYSA-N	261789-00-8
MDAI	5,6-Methylenedioxy-2-aminoindane	6,7-dihydro-5H-indeno[5,6-d]-1,3-dioxol-6-amine	DEZYWEZDXRXACY-UHFFFAOYSA-N	344-90-4
2-AI	2-Aminoindane	2,3-dihydro-1H-inden-2-amine	XEHNLVMHWYPNEQ-UHFFFAOYSA-N	2338-18-3

Common Name	Synonyms	Systematic Name	InChI Key	CAS Number (if applicable)
BZP	1-Benzylpiperazine	1-(phenylmethyl)-piperazine	BBUJLUKPBBBXMU-UHFFFAOYSA-N	5321-63-1
TFMPP		1-[3-(trifluoromethyl)phenyl]-piperazine	JCUKFOWDFVZILY-UHFFFAOYSA-N	76835-14-8

Table A - 3 Analyses Completed

Compound	GC-MS Added to Forendex	Smoke Condensate	Pyrolysis at 800˚C	Pyrolysis 200-800˚C	Degradation	In vitro Metabolism	In vivo metabolism	Receptor Binding
JWH-018	X	X	X	X	X	X	X	
AM-2201	X	X	X	X	X	X	X	
MAM-2201	X		X	X	X			
EAM-2201	X		X	X	X			
JWH-018 adamantyl analog	X		X	X	X	X		
JWH-018 adamantyl carboxamide	X		X	X	X	X		
STS-135	X		X	X	X			
AKB48	X		X	X	X			
UR-144	X	X	X	X	X	X	X	X
UR-144 degradant	X					X	X	X
5-Bromo-UR-144	X		X	X	X			
5-Chloro-UR-144	X		X	X	X			
XLR-11	X	X	X	X	X	X	X	X
XLR-11 degradant	X					X	X	X
XLR-11 N-(4-pentenyl) analog	X		X	X	X			
A-834,735	X		X	X	X	X		
A-834,735 degradant	X					X	X	
PB-22	X	X	X	X	X	X		X
PB-22 3-carboxyindole							X	X
5F-PB-22	X	X	X	X	X	X		
FUB-PB-22	X		X	X	X	X		
FDU-PB-22	X		X	X	X	X		
BB-22	X		X	X	X	X		
ADBICA	X		X	X	X	X		
AB-PINACA	X		X	X	X	X	X	
5F-AB-PINACA	X		X	X	X	X		
5-Chloro-AB-PINACA	X		X	X	X	X		
ADB-PINACA	X		X	X	X	X		
AB-CHMINACA							X	
AB-FUBINACA	X		X	X	X	X		
ADB-FUBINACA	X		X	X	X	X		
THJ 018	X		X	X	X	X		
THJ 2201	X		X	X	X	X		
AM2201 benzimidazole analog	X		X	X	X	X	X	

Compound	GC-MS Added to Forendex	Smoke Condensate	Pyrolysis at 800˚C	Pyrolysis 200-800˚C	Degradation	In vitro Metabolism	In vivo metabolism	Receptor Binding
THJ	X		X	X	X	X		
5F-THJ	X		X	X	X	X		
EG-018							X	
SDB-006	X		X	X	X	X		
Flephedrone					X			
α-Ethylaminopentiophenone								
NRG-3					X			
4-MeO-α-PVP								
4-MePPP					X			
α-PVT					X			
25I-NBOME					X			
2C-N					X			
MDAI					X			
2-AI					X			
BZP					X			
TFMPP					X			

Methods

Chemicals and Materials

Reference standards were purchased from Cayman Chemical (Ann Arbor, MI), Cerilliant (Round Rock, TX), Grace (Deerfield, IL) or from the original JWH synthesized compounds from John W. Huffman (Clemson University, Clemson, South Carolina) and provided by Dr. Jenny L. Wiley (RTI International, RTP, NC). PB-22 and 5F-PB22 were obtained from Hangzhou Trylead Chemical Technology Co., Ltd (Hangzhou, China). Compounds tested in vivo were obtained from the National Institute on Drug Abuse (NIDA, Bethesda, MD) through the NIDA Drug Supply Program, Cayman Chemical, and the United States Drug Enforcement Administration (DEA). Human CB1 and CB2 membrane preparations were purchased from Perkin Elmer (Waltham, MA) isolated from a HEK-293 expression system. All reagents were high-performance liquid chromatography (HPLC) grade. Acetonitrile and methanol were obtained from Fisher Scientific (Fair Lawn, NJ). Water was purchased from EMD Chemical (Gibbstown, NJ). Ammonium acetate, formic acid, glacial acetic acid, and Helix pomatia β-glucuronidase were purchased from Sigma Aldrich (St. Louis, MO). Red Abalone (*Haliotis rufescens*) β-glucuronidase was obtained from Kura Biotec (Inglewood, CA) and spin filters (0.22 μM) were obtained from Agilent Technologies Inc. (Cedar Creek, TX). Male ICR mice were purchased from Harlan Laboratories (Indianapolis, IN).

Stability/Forced Degradation

UR-144 and XLR-11 were degraded at a higher temperature than the neat compound after being aliquoted in methanol and then evaporated to dryness. At each appropriate time point, 10-40 μL (initial concentration dependent) were removed and combined with 960-990 μL organic solvent for a targeted final solution at 10 μg/mL. Samples were placed in a -80°C freezer until

analysis, at which point all samples were thawed, vortexed, and analyzed via LC-MS to detect and identify synthetic cannabinoid degradation products.

Liquid chromatography was carried out using an Acquity BEH C18 column (1.7µm X 2.1 X 50 mm). A gradient elution method with a flow rate of 400 µL/min was used with mobile phase A consisting of water with 0.1% formic acid and mobile phase B consisting of methanol with 0.1% formic acid. Injection volumes were 5 µL. Additional LC-MS methods were used for samples in which nonpolar degradants appeared or negative ions were suspected.

Metabolism

In vitro

Compounds (10 µM) were incubated at 37°C in cryopreserved human hepatocytes (pool of 20 donors), with the exception of PB-22 and 5F-PB-22, which were incubated at 100 µM, and JWH-018 and AM2201 at 50 µM . An aliquot of 100 µL was removed and quenched with acetonitrile containing 0.2% acetic acid at 0, 15, 120, and 180 min (PB-22 and 5F-PB-22 stopped at 120 min). Incubation time points for JWH-018 and AM2201 were 0, 15, 60, and 120 min. A portion of each aliquot was hydrolyzed with abalone beta-glucuronidase (≥ 5,000 units) in ammonium acetate for 2 h at 60 °C. After incubation acetonitrile was added to each sample, centrifuged and filtered with 0.22 µM spin filters prior to LC-MS analysis. PB-22 and 5F-PB-22 were treated the same as the other compounds except hydrolyzed with Helix pomatia beta-glucuronidase (≥ 5,000 units) in ammonium acetate and incubated for 3.5 h at 60 °C. Non-hydrolyzed samples were centrifuged and the supernatant was removed for analysis.

In vivo

AB-PINACA (3 mg/kg), AB-CHMINACA (3 mg/kg), AM-2201 benzimidazole analog (100 mg/kg), EG-018 (30 mg/kg), XLR-11 degradant (3 mg/kg), UR-144 degradant (3 mg/kg), A-

834735 degradant (3 mg/kg), and PB-22 3-carboxyindole (30 mg/kg) were administered by i.p. injection to four male ICR mice each. JWH-018 (3 mg/kg) and AM2201 (1 mg/kg) were dosed in six mice. Dosing and extraction methods for UR-144 and XLR-11 were previously published from this project (Wiley et al, 2013). An additional two mice were treated as the control. Dosed mice were placed in metabolism cages and urine was collected over 24 hrs. Urine from mice dosed with JWH-018 and AM2201 were pooled together separately and diluted 1:3 with acetonitrile. Samples were vortexed and centrifuged for 5 min at 10,000 rcf and filtered through 0.22 micron spin filters prior to LC-MS analysis. Urine from animals dosed with the same compounds was pooled together and extracted using a salting out liquid-liquid extraction (SALLE) method prior to analysis. Twenty-five microliters of 0.4 M ammonium acetate (pH 4.5) was added to 100 µL of sample. Abalone β-D-glucuronidase (≥ 5,000 units) was added followed by vortexing. Samples were incubated for 2 h at 60°C. The reactions were stopped by addition of 200 µL of acetonitrile. Samples were vortexed and 50 µL of 5 M ammonium acetate was added as a salting out agent. Samples were vortexed and centrifuged at 10,000 x g for 5 minutes. The top aqueous layer was removed and dried down at 40°C and reconstituted with 50 µL of mobile phase.

Liquid Chromatography-Mass Spectrometry (LC-MS)

The Waters Q-TOF mass spectrometer was operated under resolution mode, positive electrospray ionization, source temperature of 150 °C, desolvation temperature of 500 °C , desolvation gas at 1,000 L/hr, capillary voltage at 3.0 kV, sampling cone at 35 V, and extraction cone at 4.3 V. The mass spectrometer was externally calibrated from 50 - 1000 Da using a sodium formate solution. Data were acquired using either MS only or a MS^E method in which low and high collision energy data are collected nearly simultaneously for every m/z. The MS^E

method consisted of one low energy function with trap collision energy (CE) of 4 eV, and one high energy function with a trap CE ramp from 15 to 40 eV.

Liquid chromatography was performed using a gradient elution with a flow rate of 500 µL/min with mobile phase A consisting of water with 0.1% formic acid and mobile phase B consisting of acetonitrile with 0.1% formic acid. See Table A-4 for the gradient elution used for each compound in this study.

Metabolynx software was used to automate the screening for expected and unexpected metabolites by their protonated ion exact mass and potential fragments at the same retention time. Automation was supplemented with manual interrogation using mass defect filtering, precursor ion and fragment ion searching techniques. All extracted ion chromatograms were extracted with a mass window of 0.02 Da unless otherwise noted.

Pyrolysis

The pyrolysis autosampler consisted of an autosampler turret, a temperature programmable "pyro-probe," a temperature programmable trap, and a heated transfer line. The pyrolysis autosampler was controlled by CDS Pyroprobe 5000 (version 4.1.11) software (CDS Analytical). Samples were introduced to the pyrolyzer by being first loaded into quartz tubes. The quartz tubes contained long rods and a quartz wool plug positioned on top of the rod. Aliquots of standard solutions delivering 8 µg of standard material were loaded into the quartz wool with a micropipettor. The tubes were dropped by the autosampler into the pyrolyzer where they were pyrolyzed in air by the "pyro-probe." Pyroylsis at 800 ˚C was carried out by setting a starting temperature of 50 ˚C. After one second the pyrolysis probe was ramped at 20˚C/sec to 800˚C where the temperature was held for 10 seconds. The resulting pyrolysis products were collected from the air stream by means of an activated charcoal trap maintained at an initial temperature of

50 ˚C. The reactant gas (air) was replaced with helium for 1.18 minutes prior to the desorption of the activated charcoal for two minutes at a temperature of 300 ˚C.

The transfer line to the gas chromatograph was set to 300 ˚C. A split injection with a ratio of 1:50 was used at 300 ˚C. The mass spectrometer was operated in full scan mode from 50-500 m/z with the EI source temperature set to 230 ˚C and the first quadrupole was kept at 150˚C. Helium quench gas in the collision cell flowed at a rate of 2.25 mL/min and nitrogen collision gas flowed at a rate of 1.5 mL/min. The transfer line to the mass spectrometer was held at 300 ˚C.

In the variable temperature pyrolysis method the pyro-probe was held at an initial temperature of 50°C for one minute, followed by a 20 ˚C per second ramp to 200 ˚C. The sample was then cooled by ambient air to 50°C and raised following the same ramp to 400 ˚C. Again the trap was cooled to 50 ˚C and then raised to 600 ˚C, then finally cooled to 50 ˚C and raised to 800 ˚C using the same temperature ramp. At the final temperature of each heating cycle, 8 minutes of exposure to the sample was allotted before desorption of the trap and transfer to the gas chromatograph for separation of volatile products and detection by mass spectrometry.

Samples were collected at 50 ˚C in the trap and then desorbed to the GC column at 200 ˚C for the 200 ˚C injection and 350 ˚C for all others. The GC method for variable temperature analysis started at 40 ˚C and held for 1 minute. The temperature was then increased by 10˚/minute to 300 ˚C and held for 9 minutes after which the temperature was increased to 325 ˚C at 15˚/minute and held for 6 minutes. The mass spectrometer scanned from 50-500 m/z though later runs the window was expanded to 50-750 m/z in the event that a dimer would appear. All other parameters were consistent with the 800 ˚C method listed previously.

Smoking

Herbal cigarettes were prepared in triplicate from marshmallow leaf herbal material laced with one of a series of fluorinated synthetic cannabinoids and their non-fluorinated analogs: AM-2201, JWH-018, UR-144, XLR-11, 5-fluoro-PB-22, or PB-22. The triplicate cigarettes were smoked using a Borgwaldt KC smoking machine. Mainstream and sidestream smoke condensates were collected and remaining un-smoked butts were also recovered and extracted. All samples were analyzed by LC-MS using a Waters Synapt G2 Q-TOF high-resolution mass spectrometer and GC-MS using either an Agilent 5973 or an Agilent 7001B triple quadrupole system. Smoke from control cigarettes containing only marshmallow leaf was also collected for comparison to the laced cigarette samples. Appropriate reference standards were prepared and analyzed to confirm identity and determine recovery.

Receptor Binding

Affinity and efficacy at CB1 and CB2 receptors were measured. Affinity was measured using competitive displacement of [^{3}H]-CP55,940. Binding was initiated with the addition of 40 fmol of cell membrane proteins to polypropylene assay tubes containing [^{3}H] CP55,940 (ca.130 Ci/mmol) or [^{3}H]-rimonabant (ca. 26.8 Ci/mmol), a test compound, and a sufficient quantity of buffer A (50 mM Tris-HCl, 1mM EDTA, 3mM $MgCl_2$, 5mg/mL BSA, pH 7.4) to bring the total incubation volume to 0.5 mL. The concentrations of [^{3}H]CP55,940 and [^{3}H]rimonabant were 7.2 nM and 2 nM, respectively. Nonspecific binding was determined by the inclusion of 10 mM unlabeled CP55,940, or rimonabant. All cannabinoid analogs were prepared by suspension in buffer A from a 10 mM ethanol stock. Following incubation at 30 °C for 1 h, binding was terminated by vacuum filtration through GF/C glass fiber filter plates (Perkin Elmer), pretreated in 0.1% (w/v) PEI for at least 1 h. Reaction vessels were washed three times with 2 mL of ice

cold buffer B (50 mM Tris-HCl, 1 mg/mL BSA). Filter plates were air-dried and sealed on the bottom. Liquid scintillate was added and the top sealed. After incubating for 30 min, radioactivity was determined by liquid scintillation spectrometry.

Efficacy was determined using G-protein coupled signal transduction (GTP-γ-[^{35}S]) binding assays. Assay mixtures contained test compound (0.01 nM−10 μM), GDP (20 μM), GTP-γ-[^{35}S] (100 pM), and the desired membrane preparation (0.4 pM) in assay buffer (50mM Tris-HCl, pH 7.4, 1mM EDTA, 100mM NaCl, 3mM $MgCl_2$, 0.5% (w/v) BSA). Nonspecific binding was determined in the presence of 100 μM unlabeled GTP-γ-S, and basal binding was determined in the absence of a test compound. Samples were incubated with shaking for 1 h at 25°C, and the assays were terminated by filtration under vacuum. Microscint 20 was added, and filter-bound radioactivity was counted on a Packard scintillation counter.

Table A - 4 LC Gradients for Metabolite Identification

Compounds	Gradient
In vitro PB-22 and 5F-PB-22, JWH-018, and AM2201. In vivo JWH-018 and AM2201.	The gradient was held at 90% A for 0.5 min and decreased to 5% A linearly over 10 min, increased to 90% A in 0.1 min and held at 90% A for 2.9 min for column re-equilibrium.
In vitro UR-144, UR-144 degradant, XLR-11, and XLR-11 degradant. In vivo EG018	The gradient was held at 90% A for 0.5 min and decreased to 65% A over 1 min and 35% A linearly over 13 min, decreased to 5% A over 5 min and held at 90% 2.9 min for column re-equilibrium.
In vitro ADBICA, AB-PINACA, 5F-AB-PINACA, 5Cl-AB-PINACA, ADB-PINACA, AB-FUBINACA, and ADB-FUBINACA. In vivo AB-PINACA and AB-CHMINACA	The gradient was held at 90% A for 1.5 min and decreased to 55% A linearly over 15 min, decreased to 5% A over 3 min and held at 90% 2.9 min for column re-equilibrium.
In vitro JWH-018 adamantyl analog, JWH-018 adamantyl carboxamide, A-834735, A-834735 degradant, and BB-22. In vivo UR-144 degradany, XLR-11 degradant, A-834735 degradant, and PB-22 3-carboxy indole. Spice material	The gradient was held at 90% A for .5 min and decreased to 75% A over 1 min and 35% A linearly over 15 min, decreased to 5% A over 3 min and held at 90% 2.9 min for column re-equilibrium.
In vitro SDB-006, THJ, 5F-THJ, THJ-018, THJ2201, AM2201 benzimidazole analog, FUB-PB-22, and FDU-PB-22. In vivo am2201 benzimidazole.	The gradient was held at 90% A for .5 min and decreased to 85% A over 1 min and 35% A linearly over 15 min, decreased to 5% A over 3 min and held at 90% 2.9 min for column re-equilibrium.

Table A - 5 Stability/Forced Degration Results

Note: O-no degradation observed, X-degradation observed, ppt-inconclusive due to precipitation

Compound	Organic Solvent	50:50 Organic:H_2O	50:50 Organic: 0.1N NaOH	50:50 Organic : 0.1N HCl	50:50 Organic: 3%H_2O_2	Elevated Temp (~50C)
5F-PB-22	ACN	O	X	O	O	O
5F-PB-22	DMSO	X	ppt	O	X	X
A-834735	ACN	O	O	O	O	O
AB-FUBINACA	MeOH	O	O	O	O	O
AB-FUBINACA	ACN	O	O	O	O	O
AB-PINACA	ACN	O	O	O	O	O
ADBICA	ACN	O	O	X	X	X
ADBICA	MeOH	O	O	X	O	O
BB-22	ACN	O	X	O	O	O
BB-22	MeOH	X	X	O	X	X
JWH-018 Adamantyl Analog	ACN	O	O	O	O	O
JWH-018 Adamantyl Analog	MeOH	ppt	ppt	ppt	ppt	ppt
JWH-018 Adamantyl Carboxamide	ACN	X	O	O	ppt	O
UR-144	MeOH	O	O	O	ppt	X (105C)
XLR-11	MeOH	O	O	O	O	X (105C)
PB-22	ACN	O	X	O	ppt	O
XLR-11	ACN	O	O	O	ppt	O
UR144	ACN	O	O	O	ppt	O
UR144	MeOH	O	O	O	ppt	X (105C)
MAM-2201	MeOH	O	O	O	O	O
EAM-2201	MeOH	O	O	O	O	O
STS-135	MeOH	O	O	O	O	O
UR144 5-Bromopentyl	MeOH	O	X	O	O	X
XLR11 4-Pentenyl	MeOH	O	O	O	O	O
UR-144 5-Chloropentyl	MeOH	O	O	O	O	O
AKB48 (APINACA)	MeOH	O	O	O	O	O
THJ 2201	MeOH	O	X	O	O	O
AM2201 benzimidazole analog	MeOH	X	X	X	X	X
THJ 018	MeOH	O	O	O	O	O
THJ	MeOH	X	O	O	O	O
5-fluoro THJ	MeOH	O	O	O	O	O
5-chloro AB-	MeOH	O	X	O	O	X

Compound	Organic Solvent	50:50 Organic:H_2O	50:50 Organic: 0.1N NaOH	50:50 Organic : 0.1N HCl	50:50 Organic: 3%H_2O_2	Elevated Temp (~50C)
PINACA						
5-fluoro AB-PINACA	MeOH	O	X	X	O	O
ADB-FUBINACA	MeOH	O	ppt	ppt	ppt	ppt
FDU-PB-22	MeOH	X	X	ppt	O	O
FUB-PB-22	MeOH	X	X	O	X	X
SDB-006	MeOH	O	O	O	X	O
ADB-PINACA	MeOH	O	O	O	O	O
4-Methoxy-α-pyrrolidinopentiophenone (HCl)	MeOH	O	O	O	X	O
α-Ethylaminopentiophenone (HCl)	MeOH	O	X	O	O	X
α-PVT (HCl)	MeOH	O	O	O	X	O
NRG-3	MeOH	O	ppt	O	X	X
4-Fluoromethcathinone (HCl)	MeOH	O	ppt	O	O	X
4-methyl-α-pyrrolidinopropiophenone	MeOH	O	ppt	O	X	O
25I-NBOMe	MeOH	O	O	O	O	O
2C-N	MeOH	O	O	O	O	O
Benzylpiperazine (BZP) - need HILIC Method	MeOH					
2-Aminoindane	MeOH	O	O	O	O	O
Trifluoromethylphenylpiperazine (TFMPP)	MeOH	O	O	O	X	O
5,6 methylenedioxy-2-aminoindane	MeOH	O	O	O	O	O

Table A - 6 Pyrolysis at 800 ˚C Results

Compound	Area Sum %		
	Parent	Ring-opened Analog	Dehalogenated Analog
THJ-018	98		
JWH-018	91		
JWH-018 Adamantyl Analog	85		
JWH-019	84		
AM2201 Benzimidazole Analog	80		5
AKB48	74		
5F-AKB48	74		5
AM2201	70		21
MAM2201	67		15
THJ	65		
THJ-2201	63		23
JWH-122	56		
AB-PINACA	41		
EAM2201	41		17
SDB-006	34		
JWH-018 Adamantyl Carboxamide Analog	26		
AB-FUBINACA	18		
STS-135	17		15
UR-144	14	66	
ADB-FUBINACA	12		
ADB-PINACA	11		
5-Fluoro AB-PINACA	10		
5-fluoro THJ	8		10
XLR11	8	70	12
UR-144 5-Chloropentyl Analog	7	80	5
XLR11 4-Pentenyl Analog	6	83	
FDU-PB-22	3		
UR-144 5-Bromopentyl Analog	3	56	5
A-834735	2	54	
5-Chloro AB-PINACA	1		
PB-22	0		
5F-PB-22	0		
BB-22	0		
ADBICA	0		
FUB-PB-22	0		

Table A - 7 Summary of ADBICA, ADB-FUBINACA, AB-FUBINACA, ADB-PINACA, AB-PINACA, 5F-AB-PINACA, and 5Cl-AB-PINACA in vitro metabolites.

	ADBICA		ADB-FUBINACA		AB-FUBINACA		ADB-PINACA		AB-PINACA		5F-AB-PINACA		5Cl-AB-PINACA	
	I	II	I	II	I	II	I	II	I	II	I	II	I	II
Parent	X		X		X		X		X		X		X	
Hydroxylation	X	X	X		X		X	X	X		X		X	
Dihydroxylation							X							
Desaturated Hydroxylation	X		X				X		X					
Carboxylation	X						X		X					
N-dealkylation	X													
Desaturation	X													
Unknown	X													
Hydrolysis (amide, distal)			X	X	X	X	X		X	X	X	X	X	X
Hydrolysis (amide, distal) + hydroxylation							X		X	X				
Hydrolysis (amide, distal) + carboxylation									X					
Dehalogenation + hydroxylation											X		X	
Dehalogenation + Carboxylation											X		X	
Dehalogenation + Hydrolysis (amide, distal) + Hydroxylation											X			
Dehalogenation + Hydrolysis (amide, distal) + Carboxylation											X		X	X

Table A - 8 Summary of in vitro metabolites of PB-22, 5-F-PB-22, BB-22, FDU-PB-22, and FUB-PB-22 and in vivo metabolites of PB-22 3-carboxyindole excreted in urine.

	PB-22		5-F-PB-22		BB-22		FDU-PB-22		FUB-PB-22		PB-22 3-carboxyindole	
	I	II	I	II	I	II	I	II	I	II	I	II
Parent	X		X		X		X		X			
3-carboxyindole	X	X	X	X	X	X	X	X	X	X	X	X
Hydroxylated 3-carboxyindole		X			X	X				X	X	
Hydrated 3-carboxyindole					X							
Hydroxylation	X											
Carboxylation												
Transesterfication					X							
Defluorination to hydroxylation			X	X								
Defluorination to carboxylation			X	X								
Defluorinated 3-carboxyindole			X									

Table A - 9 Summary of SDB-006, JWH-018 adamantyl analog and JWH-018 adamantyl carboxamide in vitro metabolites.

	SDB-006		JWH-018 adamantyl analog		JWH-018 adamantyl carboxamide	
	I	II	I	II	I	II
Parent	X		X		X	
Hydroxylation	X	X	X	X	X	X
Dihydroxylation			X	X	X	X
Trihydroxylation					X	
Carboxylation	X		X	X		
Dihydroxylation + desaturation			X	X	X	X
Carboxylation + hydroxylation					X	
Desaturated hydroxylation	X		X		X	
Dihydrodiol	X					
Desaturation			X		X	
3-carboxamide indole	X					
N-dealkylation	X		X		X	

Table A - 10 Summary of THJ, 5F-THJ, THJ-018, THJ2201, and AM2201 benzimidazole analog in vitro (X) metabolites and in vivo (O) metabolites for AM2201 benzimidazole analog excreted in urine.

	THJ		5F-THJ		THJ-018		THJ2201		AM2201 benzimidazole analog	
	I	II	I	II	I	II	I	II	I	II
Parent	X		X		X		X		X O	
Hydroxylation	X	X	X	X	X	X	X	X	X O	X O
Saturation							X		X O	X
Trihydroxylation					X					
Carboxylation					X					
Hydration					X	X			X O	X O
Desaturated hydroxylation	X		X		X					
Dihydrodiol	X		X		X		X	X	X O	X O
Dihydrodiol+saturation									X	
Desaturation					X				X	
Defluorination + hydroxylation			X	X			X	X	X O	X O
Defluorination + hydration									X	X
Defluorination + dihydroxylation			X	X						
Defluorination + trihydroxylation										
Defluorination + carboxylation			X	X			X	X	X O	X
Defluorination + hydroxylation + carboxylation			X	X					X O	
Defluorination + carboxylation + saturation									X O	X

Table A - 11 Summary of cyclopropyl ketone indole in vitro (X) metabolites for degradant and non-degradant compounds and in vivo (O) metabolites excreted in urine for just the degradant compounds.

	XLR-11		XLR-11 degradant		UR-144		UR-144 degradant		A-834735		A-834735 degradant	
	I	II	I	II	I	II	I	II	I	II	I	II
Parent	X		X O		X		X O		X		X O	
Hydroxylation	X	X	X O	X O	X	X	X O	X O	X	X	X O	X O
Dihydroxylation			X O	X O	X	X	X O	 O	X		X O	 O
Trihydroxylation											X O	
Carboxylation					X		X O		X		X O	 O
Desaturated hydroxylation							X		X		X	
Desaturation					X		X					
N-dealkylation	X		X		X		X					
Defluorination + hydroxylation	X	X	X	X O								
Defluorination + dihydroxylation	X		X									
Defluorination + carboxylation	X		X O	X								
Defluorination + hydroxylation + carboxylation	X		X O									

Table A - 12 Conference Presentations

Title	Authors	Location
Pyrolysis Studies of Synthetic Cannabinoids in Herbal Products	Richard C. Daw, Megan Grabenauer, Poonam G. Pande, Anderson O. Cox, Alexander L. Kovach, Kenneth H. Davis, Jenny L. Wiley, Peter R. Stout, Brian F. Thomas	College on Problems of Drug Dependence (CPDD) June 15-20, 2013 in San Diego, CA
Analysis of Smoke Condensate from Combustion of Synthetic Cannabinoids in Herbal Products	Brian F. Thomas, Richard C. Daw, Poonam G. Pande, Anderson O. Cox, Alexander L. Kovach, Kenneth H. Davis, Megan Grabenauer	Poster presented at the 23rd Annual International Cannabinoid Research Society (ICRS) Symposium on the Cannabinoids June 21-26, 2013 in Vancouver, British Columbia, Canada
Identification of In Vivo and In Vitro Metabolites of UR-144 and XLR-11 by UPLC-QTOF Mass Spectrometry	Katherine N. Moore, Timothy W. Lefever, Jenny L. Wiley, Julie A. Marusich, Brian F. Thomas, Megan Grabenauer	Society of Forensic Toxicologists (SOFT) meeting October 28 – November 1, 2013 in Orlando, FL
Analysis of Smoke Condensate from Herbal Cigarettes Laced with Fluorinated Synthetic Cannabinoids	Brian F. Thomas, Alex L. Kovach, Anderson O. Cox, Richard C. Daw, Megan Grabenauer	Society of Forensic Toxicologists (SOFT) meeting October 28 – November 1, 2013 in Orlando, FL
Degradation of Synthetic Cannabinoids UR-144, XLR-11, PB-22, and 5F-PB-22 Analyzed by UPLC-QTOF Mass Spectrometry	Megan Grabenauer, Alexander L. Kovach, and Brian F. Thomas	Poster presented at the American Academy of Forensic Sciences (AAFS) meeting February 17 – 22, 2014 in Seattle, WA
Identification of In Vitro Metabolites of PB-22 and 5F-PB-22 by UPLC-QTOF Mass Spectrometry	Katherine N. Moore, Brian F. Thomas, and Megan Grabenauer	Poster presented at the American Academy of Forensic Sciences (AAFS) meeting February 17 – 22, 2014 in Seattle, WA
Major Metabolites of Structurally Related Cannabimimetic Compounds by UPLC-QTOF Mass Spectrometry	Katherine N. Moore, Brian F. Thomas, Megan Grabenauer	Poster presented at the Society of Forensic Toxicologists (SOFT) meeting October 19 – October 24, 2014 in Grand Rapids, MI
Identification and Characterization of Synthetic Cannabinoid Pyrolysis Products	Megan Grabenauer, Brian F. Thomas, Anderson O. Cox, Alexander L. Kovach, Jenny L. Wiley, Ann M. Decker, Elaine A. Gay	Poster presented at the Society of Forensic Toxicologists (SOFT) meeting October 19 – October 24, 2014 in Grand Rapids, MI